J Electr Eng Technol.2017; 13(?): 1921-718
http://doi.org/10.???/JEET.2017.13.1.1921

ISSN(Print) 1975-0102
ISSN(Online) 2093-7423

Active Distribution System Planning Considering Battery Swapping Station for Low-carbon Objective using Immune Binary Firefly Algorithm

Ji-Ying Shi*, Ya-Jing Li*, Fei Xue†, Le-Tao Ling*, Wen-An Liu, Da-Ling Yuan* and Ting Yang ***

Abstract – Active distribution system (ADS) considering distributed generation (DG) and electric vehicle (EV) is an effective way to cutting carbon emission and improving system benefits. ADS is an evolving, complex and uncertain system, thus comprehensive model and effective optimization algorithms are needed. Battery swapping station (BSS) for EV service is an essential type of flexible load (FL). This paper establishes ADS planning model considering BSS firstly for the minimization of total cost including feeder investment, operation and maintenance, net loss and carbon tax. Meanwhile, immune binary firefly algorithm (IBFA) is proposed to optimize ADS planning. Firefly algorithm (FA) is a novel intelligent algorithm with simple structure and good convergence. By involving biological immune system into FA, IBFA adjusts antibody population scale to increase diversity and global search capability. To validate proposed algorithm, IBFA is compared with particle swarm optimization (PSO) algorithm on IEEE 39-bus system. The results prove that IBFA performs better than PSO in global search and convergence in ADS planning.

Keywords: Active distribution system planning, Low carbon, Distributed generation, Flexible load, Battery swapping station, Immune binary firefly algorithm

1. Introduction

Global warming and declining resources are significant challenges of our social society. Fossil-fuel CO_2 is regarded as a chief cause of global warming. Curbing the CO_2 emission suppresses the pressure from environmental pollution and energy shortage. Distributed generation (DG) and electric vehicle (EV) taxis develop rapidly with their low carbon emissions and flexible operation mode. But the complexity and uncertainty of the system increase greatly when a considerable amount of DG is connected into the distribution network. And the connection of DG leads to bidirectional power flows, which makes the distribution network active. Therefore active distribution system (ADS) is put forward. And it is thought as an effective solution to realize the flexible operation of the distribution networks [1, 2].

Lots of researches on distribution system planning considering DG have been done. Ref. [3] optimizes DG sizing and sitting in a smart distribution power system to maximize the benefit to cost ratio. Ref. [4] established the expansion planning model of network based on DG, using scenario analysis to deal with the uncertainties of DG and flexible load (FL). Ref. [5] aims at increasing DG penetration with the purpose of best coordinating the target of renewable energy harvest with the benefits of individuals. To maximize DG energy utilization, FL is a viable option for enabling the integration of intermittent DG energy [6]. EV taxis are considered as an essential component of FL. Ref. [7] proposes a stochastic modeling method of the plug-in EV distribution, and analyzes its effects on power systems at different penetration levels. Ref. [8] discusses the planning solution of EV integration in fast charging battery system. Ref. [9] deals with the collaborative planning issue in EV charging station systems and integrated power distribution. In all aforementioned works, plug-in EV charging strategies are mostly discussed in ADS planning, whereas battery swapping station (BSS) is seldom mentioned. BSS realizes the decoupling of EV and batteries, which simplifies the decision variables, battery investment and management, and charge-discharge dispatch. It is thought to be time-saving for consumers, profitable for BSS operators, and convenient in power dispatch for power companies. BSS management system has already developed in many countries, such as Israel, France and etc. [10]. Plenty of interest has been towards BSS. Ref. [11] analyzes the basic frame, operation mode and management system of battery-swapping network. Ref. [12] presents a stochastic model to estimate energy consumption of the BSS. Ref. [13] proposes a model for the optimal planning of BSS, including locations, sizes,

† Corresponding Author: Electric Power Research Institute, State Grid Ningxia Electric Power Company, China. (tjuxf1010@126.com)
* Dept. of Electrical and Electronic Engineering, Tianjin University, China. ({eesjy, daling_yuan}@163.com, tjulyj110@126.com, lingloktou@gmail.com, gildong@kiee.or.kr)
** ZiBo Power Supply Company, State Grid Shandong Electric Power Company, China. (liuwenan515@126.com)
Received: March 30, 2017; Accepted: October 10, 2017

and charging strategies. Ref. [14] contains BSS in smart grid dispatch, where BSS is used to stabilize the wind power output variability and uncertainty. And this paper first considers the influence of BSS in ADS planning.

ADS planning is a discrete, nonlinear and mufti-objective optimization problem. Intelligent algorithms are effective optimization methods, such as particle swarm optimization (PSO) algorithm [15], genetic algorithms [16], bacterial foraging algorithm [17], quantum artificial fish swarm algorithm [18], ant colony algorithm [19], biogeography optimization algorithm [20], bacterial colony chemotaxis algorithm [21], etc. PSO is one of the most classical algorithms in ADS planning, which is a benchmark for new algorithms. Firefly algorithm (FA) is a neotype of intelligent algorithms. It performs well in global searching, simple structure, and faster convergence [22]. Based on FA, immune binary firefly algorithm (IBFA) is put forward. Antibody concentration is considered via updating which is inspired by biological immune mechanism. Population diversity is preserved and global searching ability is improved.

The remainder of the paper organized as follows. Firstly, planning models and the problem formulations, as well as demand response (DR), scenario synthesis, are introduced in Section 2. Next, section 3 proposes the solution algorithm, i.e., IBFA. Simulation results and its analysis of ADS planning on modified IEEE 39-bus power system are presented in Section 4. Finally, conclusions are drawn in Section 5.

2. ADS Planning Model

2.1 Basic structure of ADS

2.1.1 Wind generation model

Wind generation is one of the most significant DG forms. Wind speed is of great indeterminacy, and it is usually considered subject to Weibull distribution [23]. The relationship between the output of the wind turbine and the wind speed is represented as:

$$P_g^w = \begin{cases} 0 & v_g \le v_{in}^{cut} \cup v_g > v_{out}^{cut} \\ \dfrac{v_g - v_{in}^{cut}}{v_{rated} - v_{in}^{cut}} . P_{rated}^w & v_{in}^{cut} < v_g \le v_{rated} \\ P_{rated}^w & v_{rated} < v_g \le v_{out}^{cut} \end{cases} \quad (1)$$

where v_{in}^{cut} , v_{out}^{cut} and v_{rated} represent the cut-in, cut-off and rated speed of the wind turbine, respectively; P_{rated}^w is the power capacity. Eq. (1) is shown schematically in Fig. 1.

2.1.2 Battery swapping station

EV taxis have already played a vital role in transit systems under government's support [24]. Some cities in Unites States, China, South Korea, and so on, have built an integrated EV public transit system [25]. EV taxis need to charge their batteries frequently due to limited battery capacity and long travel distance, though well-behaved in green and clean energy consumption. Nevertheless, the minimum charging time to 80% is about 30 minutes when EV taxis cannot make profits [26]. What's more, EV taxi drivers intend to recharge at some fixed time slots when passenger riding requests are less and stations where EV taxi drivers can reach more easily and enjoy better treatment. Central charging challenges the stability and safety of distribution systems [25]. BSS can solve the problem well. It only takes minutes to swap batteries in BSS which saves time greatly. BSS enables the separation of asset relationships between EV and batteries, and the separation of sites and time between driving and charging, which pushes the maturity of EV market. Besides, the redundant batteries can be used to chip peak off and fill valley up, which benefits the stability and load rate of power system. In recent years, BSS has turned into a promising concept in dealing with road safety, traffic jam and energy consumption. Thus, relevant studies considering BSS in ADS planning is earnestly required. Private EV owners are more likely to charge after backing home at night, which does little help to shift the peak load and improve DG power utilization. Therefore, we only analyze the penetration of EV taxis in network planning including DG and FL in this paper.

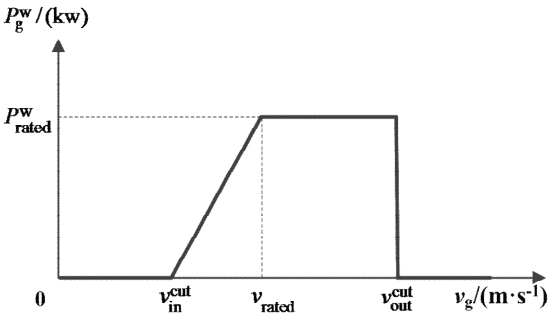

Fig. 1. Relationship between wind turbine output and wind speed

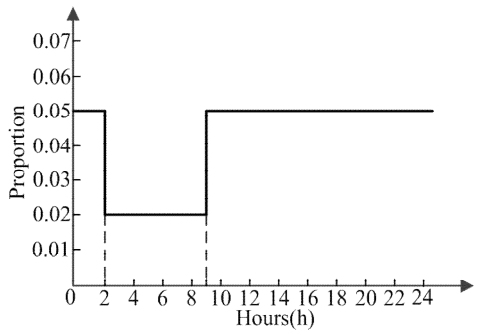

Fig. 2. The relationship of battery swapping demand at day and night

The passenger riding requests may occur at any time of a day, and they are relative low at late night and in the early morning. It can be seen from Ref. [25] that the passenger riding requests are hovering in a narrow range from 7 a.m. to 12 p.m. and from 0 a.m. to 7 a.m., respectively. Besides, the distribution of passenger riding requests is not correlated to decision variable solving methods. Therefore, this paper assumes that stochastic passenger riding requests follow piece-wise even distribution. The battery swapping demand is assumed to have a 2-hour-delay compared to the passenger riding requests. Accordingly, the battery stochastic swapping behavior can be assumed to be distributed evenly from 9 a.m. to 2 a.m. and from 2 a.m. to 9 a.m., respectively. And the ratio of battery swapping demand of 2 a.m. to 9 a.m. and the other time is assumed to be 2:5, which is almost the same as the average in [25]. The relationship of battery swapping demand at day and night can be depicted as below:

2.1.3 System structure

Wind generation connect to grid through AC/DC and DC/AC converters. BSS connects to grid through DC/DC and DC/AC converters. The output voltage of the wind system and battery storage are 380 V and 700 V, respectively. System block diagram is shown as follow:

2.2 Demand response

DR is flourishing because it helps network match up with uncertain renewable energy better. DR is the market behavior that the power consumer changes the normal power consumption pattern in response to the power system price signal or the incentive mechanism [27]. It can be categorized to two parts, time-based and incentive-based programs [28]. In Time-Of-Use (TOU) program, the electricity price fluctuates throughout the day. Peak, mid-peak and off-peak are usually referred to as three levels in this program. Real Time Price (RTP) service is related to volatility of electricity prices in 24 hours, in minutes or seconds. Critical Peak Pricing (CPP) program defines two levels of electricity prices. Incentive based programs of DR induce customers to participate in a variety of load adjustment driving by incentives for shaving or maintaining system reliability [28]. TOU program implements easily and is widely used. Therefore, it is considered in this paper.

Three levels (peak, mid-peak, off-peak) of TOU program from [29] is used and shown in Fig. 4.

Owing to the different load attributes, only parts of the load can response to the TOU program. It is assumed that participating rate is λ_{pa}.

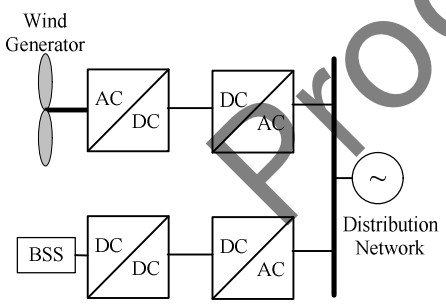

Fig. 3. System block diagram

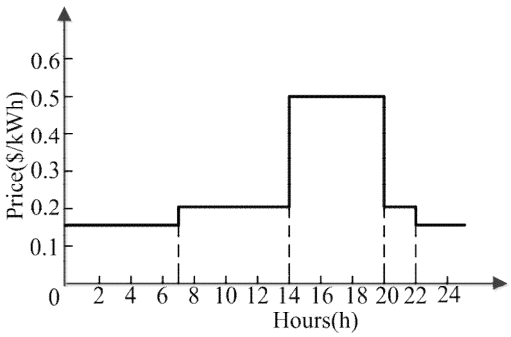

Fig. 4. Network electricity price at 24 hours a day

2.3 Scenario synthesis

The uncertainties caused by intermittent wind and uncertain FL are usually dealt with Monte-Carlo [30], the point estimation [31], scenario synthesis [32], etc. The classic scenario synthesis is used in this paper. The probability of scenarios *NS* can be presented as follow:

$$p(b) = \int_{P_{l,b}}^{P_{u,b}} \int_{v_{l,b}}^{v_{u,b}} f(D^{\mathrm{fl}}) f(v) \mathrm{d}P \mathrm{d}v \tag{2}$$

where $f(D_{\mathrm{fl}})$ and $f(\mathrm{v})$ are density function of flexible load and wind speed; $P_{\mathrm{l,b}}/P_{\mathrm{u,b}}$ and $\mathrm{v_{l,b}}/\mathrm{v_{u,b}}$ are the floor or ceiling of FL and wind speed, respectively, in scene *b*.

2.4 Objective and constrains

2.4.1 Objective function

The objective function $F(\cdot)$ is the minimum of the total economic cost. Not only the traditional costs including feeder investment, O&M expenses, network losses, but also the environmental costs due to the carbon emission of electricity generation are took into account:

$$F = C_{\mathrm{cap}} + C_{\mathrm{opr}} + C_{\mathrm{emi}} \tag{3}$$

where C_{cap} is the annual value of feeder investment; C_{opr} is the fee of network losses and O&M; C_{emi} represents the expectation value of environmental costs paid for carbon emissions. Now that DG has little carbon emissions, C_{emi} is mainly made up of carbon taxes paid for the carbon emission from generation side, which origins from network loss and customer loads overstepping total DG power. C_{cap}, C_{opr} and C_{emi} can be respectively calculated as:

$$C_{\text{cap}} = \varepsilon \sum_{i \in NF} \mathrm{c}_{\text{cap}}(m) l_i n_i^{\text{fdr}}(m) \tag{4}$$

$$C_{\text{opr}} = \sum_{t=1}^{NT} \mathrm{c}_{\text{opr}} \beta_t \sum_{b \in NS} p(b) \sum_{i \in NF} \frac{r(m) l_i \left| I_{i,b} \right|^2}{n_i^{fdr}(m)} + \sum_{i \in NF} c_{\text{om}} l_i \tag{5}$$

$$C_{\text{emi}} = \sum_{t=1}^{NT} \mathrm{c}_{\text{emi}} \beta_t \sum_{b \in NS} p(b) \left[\sum_{i \in NF} \frac{r(m) l_i \left| I_{i,b} \right|^2}{n_i^{fdr}(m)} + \sum_{j \in NB} P_{j,b}^d - \sum_{g \in NG} \left(P_{g,b}^t - P_{g,b}^{\text{curl}} \right) \right] \tag{6}$$

where NT is the number of time buckets in a year, NF is the line corridor set, NS is the expected scenario set, NB is the node set and NG is the generator set; $r(m)$, $\mathrm{c}_{\text{cap}}(m)$ and $n_{\text{i}}^{\text{fdr}}$ (m) are electrical resistivity, unite length cost and erection number of m-type line, respectively; l_i and $I_{i,b}$ represent the length of line corridor i and the current value in scenario b; ε is an annual-value operator which can be expressed by $\varepsilon=d(1+d)^T/[(1+d)^T\text{-}1]$ (d is the discount rate and T is the expected line life); β_t represents the length of time bucket t; c_{opr} and c_{om} are the network loss cost per kW and O&M fee annually, respectively; c_{emi} represents the environmental cost of CO_2, i.e., the expenditure on CO_2 emission per kW·h; $P_{j,b}^d$, $P_{g,b}^t$ and $P_{g,b}^{curl}$ represent the active loads of node j, generated energy and power cuts of DG denoted by g, respectively, in scene b. The decision variable is a piece of binary code representing the operating state of line corridors.

2.4.2 Constraints

Limit of the maximum line number, power balance constraints, line capacity constraint, node voltage constraint, terminal network and radial structure are included.

$$\begin{cases} P_{j,b} = \left|V_{j,b}\right| \sum_{k \in NB} \left|V_{k,b}\right| \left(G_{jk} \cos\theta_{jk,b} + B_{jk} \sin\theta_{jk,b} \right) \\ Q_{j,b} = \left|V_{j,b}\right| \sum_{k \in NB} \left|V_{k,b}\right| \left(G_{jk} \sin\theta_{jk,b} - B_{jk} \cos\theta_{jk,b} \right) \\ 0 \le \left|I_{i,b}\right| \le I_{\max}(m) n_i^{\text{fdr}}(m) \\ V_{\min} \le \left|V_{j,b}\right| \le V_{\max} \\ \sum_{g \in NG} \left(P_{g,b}^t - P_{g,b}^{\text{curl}} \right) \le \sum_{i \in NF} \frac{r(m) l_i \left|I_{i,b}\right|^2}{n_i^{fdr}(m)} + \sum_{j \in NB} P_{j,b}^d \\ \sum_{g \in NG} \left(P_{g,b}^t - P_{g,b}^{\text{curl}} \right) \tan\phi_g \le \sum_{i \in NF} \frac{x(m) l_i \left|I_{i,b}\right|^2}{n_i^{fdr}(m)} + \sum_{j \in NB} Q_{j,b}^d \\ 0 \le P_g^{\text{curl}} \le \omega_{\max}^{\text{curl}} P_g^t \\ \phi_{\min,g} \le \phi_g \le \phi_{\max,g} \end{cases} \tag{7}$$

where $P_{j,b}$ and $Q_{j,b}$ are active and reactive power injected to node j, respectively, in scene b; $|V_{j,b}|$ is the voltage magnitude of node j. G_{jk} and B_{jk} are the real and imaginary part of the system admittance matrix, respectively; $\theta_{jk,b}$ is the voltage phase difference between nodes j and k in scene b; $I_{\max}(m)$ and $x(m)$ are upper current limit and electrical conductivity of m-type wire respectively; Q_{jb}^d is the reactive loads power of nodes j in scene b; P_{curl}^g is active power reduction to intermittent DG; $\omega_{\max}^{\text{curl}}$ is the maximum reduced rate of active power; $\varphi_{\min,g}$ and $\varphi_{\max,g}$ are bounds of power angle.

3. Immune Binary Firefly Algorithm

3.1 Overview of firefly algorithm

Firefly algorithm (FA) is a sort of intelligent algorithm which was inspired by fireflies in nature. It was first proposed by a Cambridge scholar called Xin She yang [33]. Fireflies exchange the information to hunt or attract mates by light. The main factors attracting companions depend on the brightness itself and the attractiveness. The brightness of a firefly at a particular location is decided by encoded objective function. However, light intensity decreases as the distance from its source increases. The attractiveness among fireflies is proportional to their brightness; therefore, it decreases as the distance increases. FA is superior in few parameters, high convergence speed, ease of using, powerful global searching ability, and etc. And its effectiveness has been demonstrated in continuous and discrete interval [34]. The main flowchart of FA is listed as follows:

a) Initialize the parameters of FA, including the light absorption coefficient γ, randomization parameter α, maximum attractiveness β_0, maximum iteration numbers and firefly population.
b) Initialize fireflies' position, i.e., the decision variable.
c) Calculate the firefly objective function value, remarking as the original light intensity I_0.
d) The light intensity and the attractiveness of a firefly are formulated by Eq. (8) and Eq. (9). Rank fireflies referring to light intensity.

$$I = I_0 e^{-\gamma r_{ij}} \tag{8}$$

$$\beta = \beta_0 e^{-\gamma r_{ij}^3} \tag{9}$$

where i and j are two different fireflies, respectively.
e) The movement of firefly i, which is attracted to the more attractive firefly j is determined by Eq. (10).

$$x_i = x_i + \beta(x_j - x_i) + \alpha \otimes \varepsilon_i \tag{10}$$

where ε_i represents a random searching vector obeying a standard Gaussian distribution symbolized by N (0, 1).
f) Repeat Steps c) to e) until the maximum iteration number is reached.
g) Export the so-far-best firefly individual and the optimum value to get the final solution.

3.2 Immune binary firefly algorithm

ADS planning is a combination optimization issue. To optimize ADS planning, the discretization of FA is needed. The distance between the binary fireflies is described by Hamming distance, just as PSO does [35]. Update rate and position are updated by:

$$v_{id} = \omega v_{id} + \beta(x_{jd} - x_{id}) + \alpha \otimes \varepsilon_i \tag{11}$$

$$x_{id} = \begin{cases} 1 & rand() < S(v_{id}) \\ 0 & \text{else} \end{cases} \tag{12}$$

where *rand* (.) distributes randomly in [0, 1]. Sigmoid is a piecewise function formulated as:

$$S(v_{id}) = \begin{cases} 0.98 & v_{id} > V_{\max} \\ \dfrac{1}{1+\exp(-v_{id})} & -V_{\min} < v_{id} < V_{\max} \\ -0.98 & v_{id} < -V_{\min} \end{cases} \tag{13}$$

Fireflies update their location referring to the light intensity of all fireflies, which reduces updating efficiency. In this paper, only part fireflies, especially the outstanding ones, are chosen to be referred. In addition, the concepts of memory pool and immune algorithm are introduced to improve the search capability [36]. Memory pool stores several optimums after one-iteration. And it refreshes obeying first in first out (FIFO) principle. After a certain iteration length, the optimal in memory pool substitutes the worsen fireflies to re-update in the next generation. The immune system is composed of antigen recognition system, memory mechanism, the promotion or suppression of antibody. Antibodies produced from cell division protect human against varieties of antigens. Yet with the antibody concentration too high, allergy may happen. Through the promotion and suppression of antibodies, antibody amount can be controlled. Antibody group S contains N antibodies, which are discrete binary variables taking M distinct values.

The units labeled S_1, …, S_q, …, S_z are alleles from the j-th locus, where $\{S_1, \ldots, S_q, \ldots, S_z\} \in S$. .The information entropy of the j-th allele can be defined as:

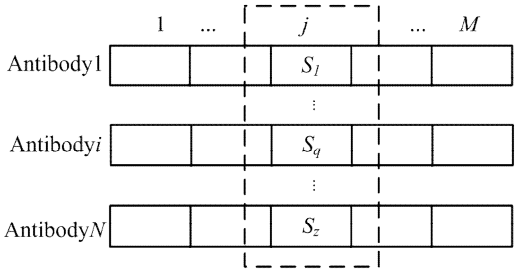

Fig. 5. The information structure of gene

$$E_j(N) = \sum_{i=1}^{N} p_{ij} \lg(1/p_{ij}) \tag{14}$$

where p_{ij} is the probability of the j-th locus being the i-th symbol. It is formulated by:

$$p_{ij} = \frac{N_{ij}}{N} \tag{15}$$

where N_{ij} is the total number of the i-th symbol in the j-th locus.

Individual diversity is represented by the average information entropy $H(N)$, defined as:

$$H(N) = \frac{1}{M} \sum_{j=1}^{M} H_j(N) \tag{16}$$

Affinity A_{ij} is the matches between antibody i and j, which is defined as:

$$A_{ij} = \frac{1}{1+H(2)} \tag{17}$$

Colony affinity is defined as:

$$A(N) = \frac{1}{1+H(N)} \tag{18}$$

The affinity with the antigen describes the antibody's fitness to the antigen and it is defined as:

$$A_i = \frac{1}{1+opt_i} \tag{19}$$

The index of antibody concentration c_i describes the proportion of antibodies whose similarity to antibody i is greater than λ. It is defined as:

$$c_i = \frac{TN_i}{N} \tag{20}$$

where λ is the similarity constant on the interval [0.9,1.0]; TN_i is the total number of antibodies whose similarity to i is greater than λ.

The selection probability of antibody i is e_i.

$$e_i = \frac{A_i}{c_i} \tag{21}$$

Rank antibodies upon e_i in decrease order. Some antibodies with less probability are replaced by reborn antibodies from memory pool. Nevertheless, the other parts of antibodies with less probability increase the updating rate by modifying their parameters. By doing so, antibodies with higher concentration and lower affinity to antigen are

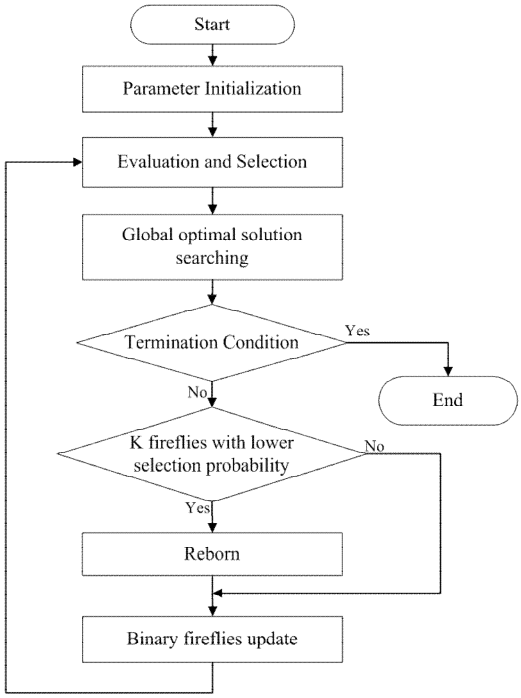

Fig. 6. The flowchart of immune binary firefly algorithm

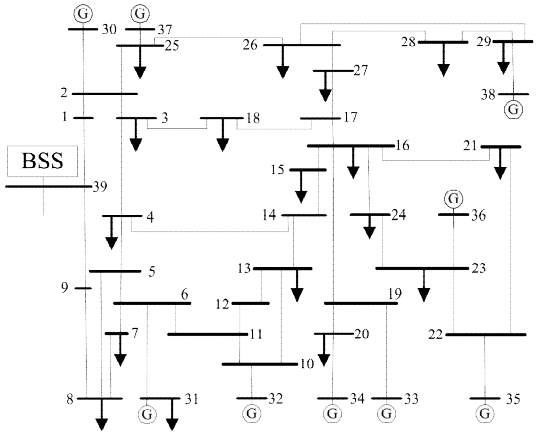

Fig. 7. Modified schematics of IEEE 39-bus system

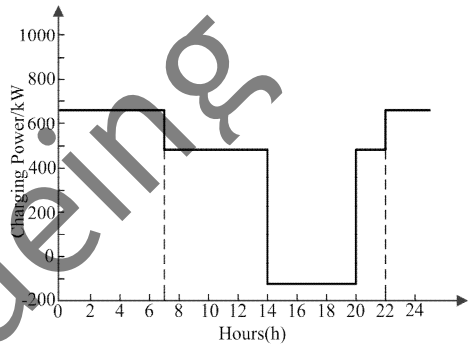

Fig. 8. The simulations run of BSS load curve

suppressed. And diversity is ensured. The main flowchart of IBFA is listed as follows:

a) Initialize the parameters of IBFA, besides those of FA, similarity constant λ, the number of fireflies saved in memory pool each-iteration and iteration length L is also included.
b) Initialize the decision variable, i.e., lines operating statues.
c) Calculate light intensity I, and store several fireflies with higher I in memory pool.
d) Calculate antibody concentration c_i and rank fireflies.
e) Substitute fireflies with lower selection probability, i.e. c_i, by the one generated randomly or the optimal stored in memory pool L-iteration ago.
f) Update binary fireflies using Eq. (11) to (13).
g) Repeat Steps c) to f) until the maximum iteration is reached.
h) Export the so-far-best firefly individual and the optimum value.

The procedure of IBFA is depicted as follow:

4. Case Study

4.1 Modified IEEE 39-bus test system

A modified IEEE 39-bus power system as shown in Fig. 7 is employed for case study. The distribution network usually works in open-loop way, thus the network need to be transformed into a radial one.

Suppose that DG access to the power grid at nodes ranging from 30 to 38, and at most 10 wind turbines are allowed to access to each node. BSS locates at node 39. The optimal solution of ADS planning is searched by changing lines running status.

The mufti-parameter settings for modules such as wind turbines and FA are displayed as follows:

Set the power base of the system as 1 MVA and the voltage deviation limit as ±6%.

v_{in}^{cut}=3m/s, v_{out}^{cut}=25m/s, v_{rated}=13m/s, k=2.3, c=8.92, P_{rated}=20kW, n_{max}^{fdr}=4, β_t=1h, T=30, d=8%, N=100, MAXGEN=100, ω=1, β_0=1.5, λ=0.9, γ=1/9500, α=1.

The feeder upgrade cost c_{cap} is \$8427/km. The carbon tax c_{emi} and grid emission intensity are taken as \$10/t and 0.92 kg (CO_2)/(kW·h), respectively [37].

Besides, it is assumed that there are 200 EV taxis, whose battery capacity is 12kWh, and every EV taxi swaps 4 times every day. The backup batteries needed are 1.5 times the vehicle they serves [38].

4.2 Simulation results and analysis

4.2.1 Load curves considering TOU program

After the adoption of TOU program, BSS operator trends to charge batteries at low power price and discharge at high power price for the sake of profit. With the consideration of

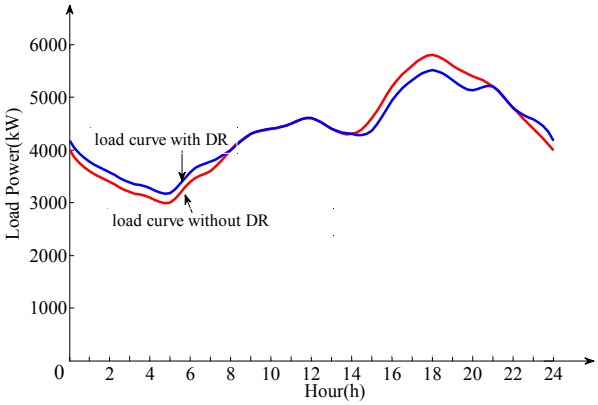

Fig. 9. Comparison of load curves with or without DR

customer requirement and the backup battery capacity, the simulation run of BSS load curve is shown below:

The typical daily load curves also change. And the comparison of load curves with or without TOU program is depicted below with the participation rate λpa=5%.

As is graphically depicted by Fig. 9, parts loads are shifted from peak to valley after the adoption of DR. Load shaping is achieved, which improves the load rate of system and decreases the equipment investment of power transmission and transformation.

4.2.2 Planning Analysis

The results of four different cases are compared in this paper:

(a) Traditional cost planning, i.e. the basic case.

(b) Same as case (a), except the consideration of low-carbon objective.

(c) ADS planning considering DG installation.

(d) Comprehensive ADS planning with DG and FL.

The optimization results of each case are tabulated in Table 1. And the cost herein is annualized.

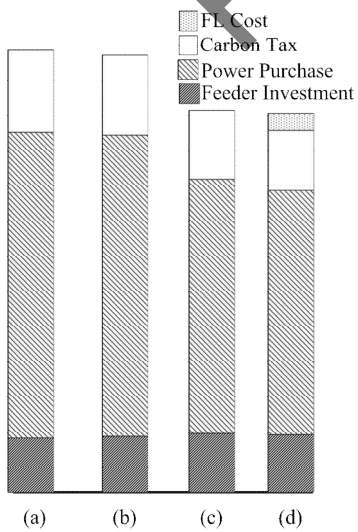

Fig. 10. Comparison of planning results between different cases

Table 1. Comparison of planning results between different cases

		(a)	(b)	(c)	(d)
Feeders investment (M $)		0.02232	0.02412	0.02585	0.02573
Operation (M $)	Power purchase	10.748	10.740	8.8132	8.7956
	Carbon tax	0.38588	0.38560	0.31642	0.31578
Net cost of FL deployment (M $)		N/A	N/A	N/A	0.0113
Total cost (M $)		11.186	11.1497	9.1555	9.1484
CO_2 emissions (t)		38588	38560	31642	31578
CO_2 reduction (%)		-	0.07	18.00	18.16

Compared with case (a), the overall interests of case (b)-(d) are improved, and CO_2 emission decreases significantly, which meets expectations.

The total cost and CO_2 emissions are 0.07% better than that of case (a). However, the network reinforcement cost of case (b) is 8.04% higher than that of the basic case. Outcome isn't accordance with income. It may work for the extraordinary role that network loss plays in the planning decision in case (b). After the consideration of network loss, ADS planning trends to choose the grid structure with smaller net loss to ensure low carbon emissions. Meanwhile, the slight curtailment of CO_2 emissions suggests that low-carbon planning, which only focuses on the net loss is unfeasible economically.

Compared with case (a), case (c) has 18.00% cost saving and CO_2 emissions reduction. It is fair to say that DG improves the system benefits both economically and environmentally by contrasting with the basic case.

With the consideration of both DG and TOU program in case (d), the overall cost and CO_2 emission are reduced by 18.166% and 18.165% even further, respectively. Apparently, without TOU program, a power curtailment may occur at night and in the early morning when the system is under-loaded. Hence, DG cannot give full play to its potential. However, TOU program based on pricing matches the availability of DR power and customer needs more closely. Peak shaving and valley filling is achieved.

Comprehensively speaking, the optimal solution of case (d) is superior. The optimal network frame structure of different cases is shown on the Fig.s below. All nodes are included. And the branch status, that ensures distribution network works in radial, is displayed.

4.2.3 Comparative analysis of IBFA and PSO

To prove the effective searching performance of IBFA, the optimal planning results of IBFA and PSO are compared. After the program of case (d) running 50 times, the statistical optimal values are tabulated in Table 2. IBFA behaves better than PSO in optimal, average and worst value. The average computational time of IBFA and PSO are 1165.76s and 917.85s, respectively. Though IBFA is a little slower than PSO, IBFA has much better searching efficiency than PSO.

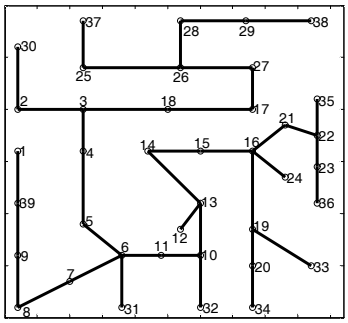

(a) Network frame structure of case (a)

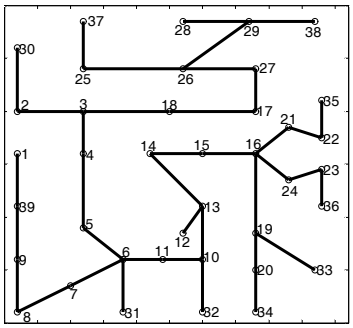

(b) Network frame structure of case (b)

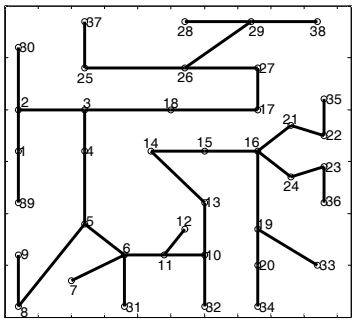

(c) Network frame structure of case (c)

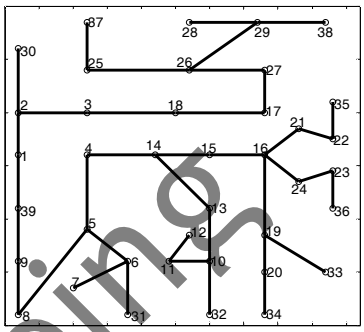

(d) Network frame structure of case (d)

Fig. 11. The optimal network frame structure of different cases

Table 2. Comparison of optimization results between different algorithms

Algorithm	Optimal value (M $)	Average value (M $)	Worst value (M $)
IBFA	0.42085	0.422803	0.42756
PSO	0.42098	0.425421	0.43451

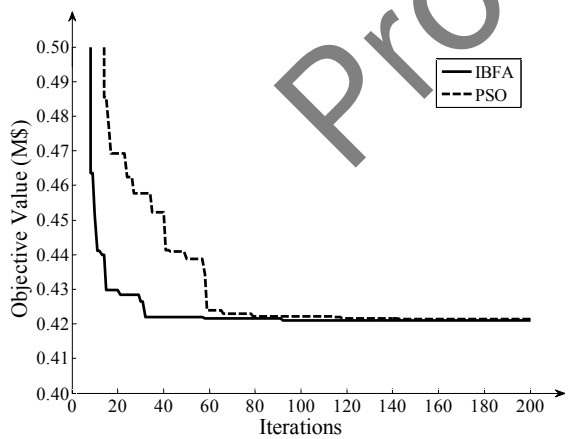

Fig. 12. Comparison of convergence between IBFA and PSO

The convergence curves of IBFA and PSO are contrasted in Fig. 12. It is observed that IBFA converges after 30 iterations, and PSO converges after 60 iterations. IBFA converges very fast in the early search stage. Therefore, IBFA has a higher converging speed. Besides, the final optimal solution of IBFA is better than that of PSO.

Memory pool and immune algorithm are introduced to improve the search capability of IBFA. Via updating, a certain number of worsen fireflies are substituted by the optimal stored in memory pool. Therefore, IBFA has more efficient searching ability and higher converging speed. Population diversity is also considered in IBFA. Antibodies with higher concentration and lower affinity to antigen are suppressed. The population is prevented from premature aging and global optimization capability is ensured. Consequently, with more efficient searching ability, higher converging speed and global optimization capability, IBFA can guarantee a better solution than PSO for all other cases.

5. Conclusion

This paper establishes ADS planning model considering DG and BSS for low carbon objective, which is optimized by newly proposed IBFA. Typical daily load curves are also simulated under TOU program. Besides, ADS planing results under four planning cases and two optimization algorithms are compared and analyzed, respectively.

It is concluded that forecasting load curve under TOU program is relatively flat, which improves system load capacity and decreases power transmission and transformation equipment investment. Simultaneously, comparisons of planning results among four planning cases demonstrate that DG and FL are effective in depressing energy wastage

and improving system efficiency overall, and they could meet the demand of rapid load increment and carbon suppression. Besides, by contrasting statistical optimal values and convergence curves between IBFA and PSO, it is testified that IBFA performs better than PSO in global searching and convergence in ADS planning.

In this paper, BSS charging demand is assumed to follow a piecewise uniform distribution. For future study, latest data can be derived for BSS load curve model establishment. Further studies on BSS charging demand could revise ADS planning model, which is conducive to real ADS planning.

Acknowledgments

This work was supported by National High Technology Research and Development Program (863 Program) (2015AA050202); National Natural Science Foundation of China (61571324); Natural Science Foundation of Tianjin (16JCZDJC30900); National Program of International S&T Cooperation (2013DFA11040).

References

[1] Y. Xiang, J. Liu and Y. Liu, "Optimal active distribution system management considering aggregated plug-in electric vehicles," *Electr. Power Syst. Res.*, vol. 131, pp. 105-115, Feb. 2016.

[2] T. Sattarpour, D. Nazarpour, S. Golshannavaz and P. Siano, "An optimal procedure for sizing and siting of DGs and smart meters in active distribution networks considering loss reduction," *J. Electr. Eng. Technol.*, vol. 10, pp. 804-811, Nov. 2015.

[3] W. Buaklee and K. Hongesombut, "Optimal DG Placement in a Smart Distribution Grid Considering Economic Aspects," *J. Electr. Eng. Technol.*, vol. 9, pp. 1240-1247, Jan. 2014.

[4] V.F. Martins and C.L.T. Borges, "Active distribution network integrated planning incorporating distributed generation and load response uncertainties," *IEEE Trans. Power Syst.*, vol. 26, pp. 2164-2172, Nov. 2011.

[5] B. Zeng, J. Wen, J. Shi, J. Zhang and Y. Zhang, "A multi-level approach to active distribution system planning for efficient renewable energy harvesting in a deregulated environment," *Energy*, vol. 96, pp. 614-624, Dec. 2015.

[6] R. Tulabing, R. Yin, N. DeForest, Y Li, K. Wang, T. Yong and M. Stadler, "Modeling study on flexible load's demand response potentials for providing ancillary services at the substation level," *Electr. Power Syst. Res.*, vol. 140, pp. 240-252.S, Nov. 2016.

[7] H. J. Son and K. S. Kook, "Stochastic Modeling of Plug-in Electric Vehicle Distribution in Power Systems," *J. Electr. Eng. Technol.*, vol. 8, pp. 1276-1282, Aug. 2013.

[8] M. Rogge, S. Wollny and D. U. Sauer, "Fast charging battery buses for the electrification of urban public transport — A feasibility study focusing on charging infrastructure and energy storage requirements," *Energies*, vol. 8, pp. 4587-4606, May 2015.

[9] X. Liu, P. Liu, and H. Zheng, "Distribution network structure planning based on QAFSA," *in 5th International Conference on Electricity Distribution*, 2012, pp. 1-4.

[10] P. H. Andersen, J. A. Mathews, and M. Rask, "Integrating private transport into renewable energy policy: The strategy of creating intelligent recharging grids for electric vehicles," *Energy Policy*, vol. 37, pp. 2481-2486, Jan. 2009

[11] C. W. Gao, X. Wu, "A survey on Battery-Swapping mode of electric vehicles," *Power Syst. Tech.*, vol. 37, pp. 891-898, Apr. 2013.

[12] Q. Dai, T Cai, S. X. Duan and F. Zhao, "Stochastic modeling and forecasting of load demand for electric bus battery-swap station," *IEEE Trans. Power Delivery*, vol. 29, pp. 1909-1917, Aug. 2014.

[13] Y. Zheng, Z. Y. Dong, Y. Xu, K. Meng, J. H. Zhao, and J. Qiu, "Electric vehicle battery charging/swap stations in distribution systems: comparison study and optimal planning," *IEEE Trans. Power Syst.*, vol. 29, pp. 221-229, Jan. 2014.

[14] Y. J. Gao, K. X. Zhao, C. Wang, Economic dispatch containing wind power and electric vehicle battery swap station, *in Transmission and Distribution Conference and Exposition* (*T&D*), *2012 IEEE PES. IEE*E, 2012, pp. 1-7.

[15] M. Hemphill, "Electricity distribution system planning for an increasing penetration of plug-in electric vehicles in New South Wales" *in Universities Power Engineering Conference*, 2012, pp. 1-6.

[16] A. Dias, P. M. S. Carvalho, P. Almeida, and S. Rapoport, "Multi-objective distribution planning approach for optimal network investment with EV charging control," *in PowerTech, 2015 IEEE Eindhoven*, 2015, pp. 1-5.

[17] G. Celli, S. Mocci, F. Pilo, G.G. Soma, R. Cicoria, G. Mauri, E. Fasciolo, and G. Fogliata, "Distribution network planning in presence of fast charging stations for EV," *in International Conference and Exhibition on Electricity Distribution*, 2013, pp. 1-4.

[18] W. Yao, J. Zhao, F. Wen, Z. Dong, Y. Xue, Y. Xu, and K. Meng, "A Multi-Objective Collaborative Planning Strategy for Integrated Power Distribution and Electric Vehicle Charging Systems," *IEEE Trans. Power Syst*, vol. 29, pp. 1811-1821, Jul. 2014.

[19] J. M. Zhu, and H. E. Ren, "A new idea for power distribution network planning using ant colony optimization," *in International Conference on Wireless Communications, NETWORKING and Mobile Computing*, 2009, pp. 1-4.

[20] P. D. Uy, "Nakagoshi N. Application of land suitability analysis and landscape ecology to urban greenspace planning in Hanoi, Vietnam," *Urban Forestry & Urban Greening*, vol. 7, pp. 25-40, Feb. 2008.
[21] P. F. Fan, L. Z. Zhang, and Z. Wang, "Improved Bacterial Colony Chemotaxis Algorithm for Distribution Network Planning," *Adv. Mater. Res.*, vol. 354-355, pp. 1002-1006, Oct. 2011.
[22] J. Wang, Z. L. Wang, J. Y. Chen, X. F. Wang, X. J. Wang and L. Tian, "A game model for DGs-loads in microgrid based on firefly algorithm and its analysis," *Auto. Electr. Power Syst.*, vol. 38, pp. 7-12, Nov. 2014.
[23] B. Zeng, J. Zhang, X. Yang, J. Wang, J. Dong and Y. Zhang, "Integrated planning for transition to low-carbon distribution system with renewable energy generation and demand response," *IEEE Trans. Power Syst.*, vol. 29, pp. 1153-1165, Dec. 2014.
[24] Y. Dong, S. Qian, J. Liu, L. Zhang and K. Zhang, "Optimal placement of charging stations for electric taxis in urban area with profit maximization," *in Software Engineering, Artificial Intelligence, Networking and Parallel/Distributed Computing (SNPD)*, 2016, pp. 177-182.
[25] Z. Tian, T. Jung, Y. Wang, F. Zhang, L. Tu, C. Xu, C. Tian, and X. Li, "Real-Time Charging Station Recommendation System for Electric-Vehicle Taxis," *IEEE Trans. Intell. Transp. Syst.*, vol. 17, pp. 3098-3109, Jan. 2016.
[26] Y. Hou, W. Zhong, L. Su, K. Hulme, A. W. Sadek and C. Qiao, "TASeT: Improving the Efficiency of Electric Taxis with Transfer-Allowed Rideshare," *IEEE Trans. Vehic. Tech.* vol. 65, pp. 9518-9528, Dec. 2016.
[27] Staff Report, "Assessment of demand response and advanced metering," *in FERC*, 2006, Docket No. AD06-2.
[28] A. Mohsenzadeh, S. Pazouki, M. R. Haghifam, and C. Pang, "Optimal planning of parking lots and demand response programs in distribution network considering power loss and voltage profile," *in Innovative Smart Grid Technologies Conference*, 2015, pp. 1-5.
[29] Y. Zheng, Z. Y. Dong, Y. Xu, K. Meng, J. Zhao, and J. Qiu, "Electric Vehicle Battery Charging/Swap Stations in Distribution Systems: Comparison Study and Optimal Planning," *IEEE Trans. Power Syst.*, vol. 29, pp, 221-229, Jan. 2014.
[30] I. S. Bae, M. K. Son and J. O. Kim, "Optimal transmission expansion planning considering the uncertainties of the power market," *J. Electr. Eng. Technol.*, vol. 5, pp. 239-245, Mar. 2010.
[31] S. Y. Lin and A. C. Lin, "Risk-Limiting Scheduling of Optimal Non-Renewable Power Generation for Systems with Uncertain Power Generation and Load Demand," *Energies*, vol. 9, pp. 868, Oct. 2016.
[32] V. F. Martins, C. L. T. Borges, "Active distribution network integrated planning incorporating distributed generation and load response uncertainties," *IEEE Trans. Power Syst.*, vol. 26, pp. 2164-2172, Apr. 2011.
[33] X. S. Yang, Nature-Inspired Metaheuristic Algorithms, Beckington: Luniver, 2010, pp. 83-96.
[34] X. S. Yang, "Firefly algorithms for multimodal optimization," *in International Conference on Stochastic Algorithms: Foundations and Applications*, 2009, pp. 169-178.
[35] J. Kennedy, and R. A. Eberhart, "A discrete binary version of the particle swarm algorithm," *in Systems, Man, and Cybernetics, 1997. Computational Cybernetics and Simulation., 1997 IEEE International Conference on*, 1997, vol. 5, pp. 4104-4108.
[36] W. Huang, C. Xu, J. Zhang, W. Huang, C. Xu, J. Zhang, and S. Hu, "Study of reactive power optimization based on immune genetic algorithm," *in Transmission and Distribution Conference and Exposition*, 2003, pp. 186-190.
[37] B. Zeng, J. Zhang, Y. Zhang, X. Yang, J. Dong, and W. Liu, "Active Distribution System Planning for Low-carbon Objective using Cuckoo Search Algorithm," *J. Electr. Eng. Technol.*, vol. 9, pp. 433-440, Mar. 2014.
[38] Y. Cai, H. Wang, Q. Ye, and M. Ouyang, "Analysis of two typical EV business models based on EV taxi demonstrations in China," *in Electric Vehicle Symposium and Exhibition*, 2013, pp. 1-6

Ji-Ying Shi He received his M.S. and Ph.D. degrees from Tianjin University. He was a Visiting Scholar and a Post-doctoral Student with The Hong Kong University of Science and Technology. He is presently working as an Associate Professor in the School of Electrical and Information Engineering, Tianjin University. His current research interests include power electronic techniques, renewable energy, and soft switching techniques.

Ya-Jing Li She received her B.S. degree in Electrical Engineering and Automation from Yanshan University. She is presently working towards her M.S. degree at Tianjin University. Her current research interests include the modeling and planning of active distribution networks, renewable energy and power electronic techniques.

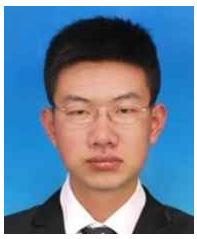

Fei Xue He received B.E and M.S degree in electrical engineering from Tianjin University. He currently is an engineer in Electric Power Research Institute, State Grid Ningxia Electric Power Company (NEPC). His research interest includes maximum power point tracking technology, renewable energy, and modeling and planning of distribution network.

Le-Tao Ling He received his B.S. degree in Electrical Engineering from Guangzhou University. Since 2015, he has been working towards his M.S. degree in the School of Electrical Engineering and Automation, Tianjin University. His current research interests include the maximum power point tracking of photovoltaic and wind power systems, renewable energy and power electronic techniques.

Wen-an Liu He received M.S degree in electrical engineering and automation from Tianjin University. He currently is working in ZiBo Power Supply Company. His research interest includes maximum power point tracking technology and modeling and planning of active distribution network.

Da-Ling Yuan She received B.E degree in electrical engineering and automation from Anhui University. She is presently working towards her M.S. degree at Tianjin University. Her research interest includes distribution network reconfiguration, location and sizing of distributed generation.

Ting Yang He is the winner of Education Ministry's New Century Excellent Talents Supporting Plan. Professor Yang is the author/co-author of four books, more than 60 publications in technical journals and conferences, and the chairman of two workshops of IEEE International Conference. He is a member of International Society for Industry and Applied Mathematics (SIAM), and a senior member of the Chinese Institute of Electronic, the committee member of electronic circuit and system. Professor Yang's research effort is focused on power electronic techniques and renewable energy.